Film Cooling on a Concave Surface: Influence of External Pressure Gradient on Film Cooling Performance

E. Lutum and J. von Wolfersdorf
ALSTOM, Business Turbomachinery, Base Development
Im Segelhof, 5405 Baden-Dättwil, Switzerland

K. Semmler and S. Naik
ALSTOM, Business Turbomachinery, GT Turbine Engineering
Haselstrasse 16, 5401 Baden, Switzerland

B. Weigand
Universität Stuttgart, Institut für Thermodynamik der Luft- und Raumfahrt
Pfaffenwaldring 31, 70569 Stuttgart, Germany

ABSTRACT

The film cooling performance on a concave surface with zero and favourable pressure gradient free-stream flow was investigated experimentally. Adiabatic film cooling effectiveness values have been obtained for five different injection geometries, three with cylindrical holes and two with shaped holes. Heat transfer coefficients were derived for selected injection configurations. Air and CO_2 injection was used to achieve a variation of the density ratio between coolant and free-stream. Free-stream acceleration caused generally an increase in adiabatic film cooling effectiveness for the investigated injection configurations and boundary conditions. This increase is stronger for the results obtained with cylindrical holes. No significant effects of the free-stream acceleration on the Stanton number ratios were obtained during corresponding heat transfer experiments. The determined heat flux ratios or film cooling performance indicated that coolant injection with shaped film cooling holes is much more efficient than with cylindrical holes especially at higher blowing rates.

NOMENCLATURE

Symbols

AR	outlet to inlet area ratio of film holes
c_p	specific heat at constant pressure
D	film hole diameter
DR	density ratio between secondary and free-stream fluid, ρ_c/ρ_g
h	convective heat transfer coefficient
I	momentum flux ratio, $(\rho_c U_c^2)/(\rho_g U_g^2)$
I_{foil}	electrical current introduced into the heating foil
K_g	acceleration parameter, $\nu_g / U_g^2 (\partial U_g / \partial S)$
L	hole length
M	blowing rate, $(\rho_c U_c)/(\rho_g U_g)$
Ma	Mach number
$\dot{q}$	specific heat flux
p	static pressure
P	total pressure
P	lateral spacing of film holes (pitch)
Pr	Prandtl number
R	radius of curved test surface
R_{foil}	specific resistance of heating foil
S	stream-wise coordinate
St	Stanton number
T	total temperature
Tu	turbulence intensity, (u'/U_g)
U	mean velocity

Greek

α	injection angle relative to the test surface
β	injection angle relative to the free-stream flow, compound angle
δ	boundary layer thickness
η_{ad}	adiabatic film cooling effectiveness
φ_1	hole extension angle in lateral direction
φ_2	hole extension angle in stream-wise direction
κ	ratio of gas specific heats
ρ	fluid density
Θ	dimensionless wall temperature

Paper presented at the RTO AVT Symposium on "Advanced Flow Management: Part B – Heat Transfer and Cooling in Propulsion and Power Systems", held in Loen, Norway, 7-11 May 2001, and published in RTO-MP-069(I).

Report Documentation Page

Form Approved
OMB No. 0704-0188

1. REPORT DATE	2. REPORT TYPE	3. DATES COVERED
00 MAR 2003	**N/A**	**-**

4. TITLE AND SUBTITLE	5a. CONTRACT NUMBER
Film Cooling on a Concave Surface: Influence of External Pressure Gradient on Film Cooling Performance	5b. GRANT NUMBER
	5c. PROGRAM ELEMENT NUMBER
6. AUTHOR(S)	5d. PROJECT NUMBER
	5e. TASK NUMBER
	5f. WORK UNIT NUMBER
7. PERFORMING ORGANIZATION NAME(S) AND ADDRESS(ES) **NATO Research and Technology Organisation BP 25, 7 Rue Ancelle, F-92201 Neuilly-Sue-Seine Cedex, France**	8. PERFORMING ORGANIZATION REPORT NUMBER
9. SPONSORING/MONITORING AGENCY NAME(S) AND ADDRESS(ES)	10. SPONSOR/MONITOR'S ACRONYM(S)
	11. SPONSOR/MONITOR'S REPORT NUMBER(S)

12. DISTRIBUTION/AVAILABILITY STATEMENT
Approved for public release, distribution unlimited

13. SUPPLEMENTARY NOTES
Also see ADM001490, presented at RTO Applied Vehicle Technology Panel (AVT) Symposium held in Leon, Norway on 7-11 May 2001, The original document contains color images.

14. ABSTRACT

15. SUBJECT TERMS

16. SECURITY CLASSIFICATION OF:			17. LIMITATION OF ABSTRACT	18. NUMBER OF PAGES	19a. NAME OF RESPONSIBLE PERSON
a. REPORT	b. ABSTRACT	c. THIS PAGE			
unclassified	**unclassified**	**unclassified**	**UU**	**16**	

Subscripts

0	without film cooling
aw	adiabatic wall
c	coolant fluid
f	with film cooling
g	free-stream fluid
inj	injection condition
la	lateral averaged
r	recovery condition
w	wall condition
TLC	Thermochromic liquid crystals

1. INTRODUCTION

The application of film cooling is required in modern gas turbine design due to high turbine inlet temperatures. Although the strength of the applied materials was improved, this high temperature and stress environment is beyond the limit alloys can presently achieve without cooling. Film cooling is used to protect the airfoil surface from high temperature of the free-stream by releasing coolant onto the surface. The coolant usually air bled from the compressor first passes internal cooling channels inside the airfoil and is afterwards injected through the surface of the hollow airfoil. Injection can be done through single or multiple rows of cylindrical holes or shaped holes.

Film cooling has been extensively studied over the past 30 years and a large body of papers is available in the open literature. A brief review of related film cooling literature that investigated the effects of wall curvature and free-stream pressure gradient was summarised in two earlier papers, i.e. Lutum et al. [1] and Lutum et al. [2]. The general trends of these investigations are:

Effects of wall curvature for cylindrical film cooling holes

- For low blowing rates the film cooling performance is increased on convex surfaces and decreased on concave surfaces compared to flat surfaces.
- For moderate blowing rates the film cooling performance is increased on convex surfaces compared to concave and flat surfaces.
- For high blowing rates the film cooling performance is increased on concave surfaces compared to convex and flat surfaces.
- The strength of the curvature effects mentioned above are more pronounced on convex surfaces.

Effects of free-stream pressure gradient for cylindrical film cooling holes

- The free-stream pressure gradient has no significant influence on the film cooling performance on flat surfaces.
- A mild adverse pressure gradient seems to have less effect than a mild favourable pressure gradient. A moderate effect occurs for strong favourable pressure gradients.
- The lateral averaged film cooling effectiveness as well as the lateral averaged heat transfer coefficient is slightly decreased due to favourable pressure gradient flow.
- The lateral spreading of the coolant fluid downstream of injection is reduced by a favourable free-stream pressure gradient.
- The effect of the free-stream pressure gradient on the heat transfer coefficient was less with CO_2 injection than with air injection.

In earlier investigations on convex surfaces by Lutum et al. [2] and Lutum et al. [3] a reduction of adiabatic film cooling effectiveness due to free-stream acceleration was obtained when compared to a zero pressure gradient flow. This was especially true in the far field downstream of coolant injection.

The present investigation gives experimental results for adiabatic film cooling effectiveness and heat transfer coefficients obtained on a concave curved surface (R/D=-150) with and without free-stream pressure gradient flow. A free-stream turbulence intensity of $Tu_g \approx 6\text{-}9\%$ at the injection location was achieved by means of a turbulence generator. The free-stream and coolant boundary conditions were systematically varied during these film cooling experiments. A zero pressure gradient flow condition at a Mach number level of $Ma_g \approx 0.2$ as well as a favourable pressure gradient flow with a constant acceleration parameter of $K_g \approx 1.0E\text{-}06$ were investigated. The current film cooling experiments were performed with air and CO_2 as coolant fluids to achieve a variation of the coolant to free-stream density ratio. The coolant blowing conditions were varied between $0.5 \leq M \leq 2.0$ for the cylindrical hole measurements and between $1.0 \leq M \leq 3.0$ for the shaped hole measurements. Film cooling

measurements have been performed with five different injection configurations, three with cylindrical and two with shaped holes.

2. EXPERIMENTAL FACILITY AND MEASUREMENT TECHNIQUE

The test facility and measurement technique used during this film cooling study was described in detail by Lutum et al. [1]. The investigation reported here focused on film cooling on a concave surface with a surface radius to film hole diameter ratio of R/D=-150, while the previous investigations were conducted with convex curvature surfaces of R/D=25 and R/D=75. Secondary fluid was injected through a single row of cylindrical or shaped holes. The multiple narrow-band thermochromic liquid crystal technique was used to determine the local wall temperature distributions along the test surface.

The concave test sections which achieved the zero and favourable free-stream pressure gradient flow conditions are shown in Fig. 1. The concave test wall was made of Necuron a low conductive polyurethane based material with a thermal conductivity of 0.1W/(mK). This wall was segmented into three parts over its height where the middle part contained the different injection configurations, which could be varied by changing this middle segment. The inner test section wall consisted of a Polycarbonat plate of 5mm thickness. Polycarbonat is a polyester based material, similar to Plexiglas, with good mechanical and optical properties. This thin Polycarbonat wall was shaped by several flexible fixations as shown in Fig. 1. This flexible inner wall design allowed moderate adjustments of the flow field in the test section. It also allowed it to be replaced by another Polycarbonat wall with a different shape, to give different free-stream boundary conditions. Both inner test section walls are shown in Fig. 1 the constant channel, which gave a zero pressure gradient flow (left graph) and the converging channel, which gave a favourable pressure gradient flow (right graph).

A total number of five film injection configurations were investigated and are shown in Fig. 2. Injection configuration CONF 1 consisted of a row of cylindrical holes. The injection angle of the film holes was α=30° relative to the surface. The holes were spaced three hole diameters in lateral direction P/D=3 and had a hole length-to-diameter ratio of L/D=7.5. The second cylindrical injection geometry CONF 2 had a lateral spacing of P/D=6. Injection configuration CONF 3 consisted of a row of cylindrical holes, which were inclined at α=30° to the surface and β=60° to the free-stream flow direction (compound angle). The lateral spacing of the holes was again P/D=6. Injection configuration CONF 4 consisted of a row of shaped holes, inclined at α=30° to the test surface. The lateral spacing of the holes was P/D=6, related to the throat diameter of the cylindrical entrance section of the shaped film holes. The cylindrical part of the hole channels had a length of 2.5 hole diameter. The remaining length of 5 hole diameters was laterally opened. An outlet to inlet area ratio of AR=3.7 was produced by the fan angle of φ_1=12°. Injection configuration CONF 5 had the same lateral extension angle φ_1 as CONF 4 and additionally a laid back angle φ_2. This streamwise widening of the film holes φ_2=15° was introduced further downstream of the cooling passages than the lateral widening and reduced the effective injection angle of the secondary fluid relative to the surface. Actually it was applied in the uncovered part of the cooling channels (see Fig. 2, CONF 5) and hence the effective area ratio was also AR=3.7.

The surface temperature data was obtained by using the narrow-band thermochromic liquid crystal technique. This measurement technique was used for both adiabatic and heat transfer film cooling measurements. Isothermal temperature patterns on the test surface were indicated by narrow-band thermochromic liquid crystals and were observed by a colour image processing system. All additional experimental data, i.e. temperature, pressure and velocity information of the free-stream and secondary flow were also recorded by this data acquisition system consisting of a personal computer using LabVIEW.

During the adiabatic film cooling experiments the temperature indications of the thermochromic liquid crystals T_{TLC} were assumed to be the local adiabatic wall temperatures T_{aw}. With the additional information of the free-stream recovery T_{rg} and secondary fluid total T_c temperatures these isothermal contour lines were transformed into adiabatic film cooling effectiveness contours η_{ad}

$$\eta_{ad} = \frac{T_{rg} - T_{aw}}{T_{rg} - T_c} . \qquad (1)$$

The recovery temperature of the free-stream flow was obtained for the turbulent external flow by using

$$T_{rg} = T_g + \left(Pr_g^{1/3} - 1\right)\frac{U_g^2}{2c_{pg}}. \quad (2)$$

In case of constant heat flux experiments with and without film cooling the thermochromic liquid crystal temperature T_{TLC} indicated the local wall temperatures T_w. For the measurements without film cooling the film cooling holes were covered with a thin aluminium tape to avoid additional sources of flow disturbances. The heat transfer coefficient in the absence of film cooling was calculated by

$$h_0 = \frac{\dot{q}_0}{T_{rg} - T_w}. \quad (3)$$

The constant heat flux $\dot{q}_0$ without film cooling was introduced by an electrical current send through the steel foil, which was glued onto the test surface. Assuming that the electrical energy introduced into the steel foil was totally transformed into heat due to foil resistance $\dot{q}_0$ was determined from

$$\dot{q}_0 = R_{foil} I_{foil}^2, \quad (4)$$

where R_{foil} is the specific foil resistance per unit area and I_{foil} is the electrical current introduced into the foil. For the experiments with film cooling the heat transfer coefficients were defined by

$$h_f = \frac{\dot{q}_f}{T_{aw} - T_w}, \quad (5)$$

where $\dot{q}_f$ is the constant heat flux with film cooling and T_{aw} is the adiabatic wall temperature. For simplicity the heat transfer experiments were conducted at iso-energetic conditions (T_c=T_g).

According to the method suggested by Moffat [4] typical experimental uncertainty values (absolute values) were determined to 0.01 for the local and to 0.011 for the lateral averaged film cooling effectiveness. Corresponding uncertainty values were determined to 4.5% for the local and to 5% for the lateral averaged heat transfer coefficient, which take into account conduction losses to the backside.

Aerodynamic experiments without coolant injection were conducted to determine the flow field quantities for the subsequently following film cooling measurements. A zero pressure gradient flow was achieved at a constant free-stream Mach number of $Ma_g \approx 0.2$ and a constant free-stream acceleration parameter of $K_g \approx 1.0E\text{-}06$ ($0.1 < Ma_g < 0.6$) was achieved in a range from S/D≈-10 to S/D≈75 as shown in Fig. 3. The boundary layer thickness at the injection location S/D=0 was $\delta/D \approx 3$ for the zero pressure gradient flow and $\delta/D \approx 2$ for the favourable pressure gradient flow. The local free-stream turbulence intensity at the injection location was $Tu_g \approx 9\%$ for the zero pressure gradient flow and $Tu_g \approx 6.3\%$ for the favourable pressure gradient flow.

3. RESULTS AND DISCUSSION

Film cooling experiments were performed for typical coolant blowing conditions with air and CO_2 injection. Four coolant mass flow rates were investigated for both free-stream boundary conditions. Blowing rates of M=0.5, 1.0, 1.5 and 2.0 were investigated for the film cooling measurements with cylindrical holes, injection configurations CONF 1 and CONF 3. Results obtained for injection configuration CONF 2 were determined at different blowing rates. The measurements with shaped holes (CONF 4 and CONF 5) were performed at M=1.0, 1,5, 2.0 and 3.0. The results obtained for zero pressure gradient flow and CO_2 injection are presented subsequently.

Results obtained with injection configuration CONF 1 shown in Fig. 4 indicate a decrease in film cooling effectiveness with increasing blowing rate for S/D<20. For streamwise distances of S/D>50 a slight increase in film cooling effectiveness with increasing blowing rate can be observed. Similar trends can also be observed for CONF 2 (Fig. 4). The film cooling effectiveness level of CONF 2 is about 50% lower compared to corresponding CONF 1 results due to the difference in the hole spacing

($P/D_{CONF\ 1}$=3 and $P/D_{CONF\ 2}$=6). The film cooling effectiveness distributions obtained with compound angle holes (CONF 3, Fig. 4) show a smaller sensitivity to a blowing rate variation compared to data for in-line injection holes (CONF 1 and CONF 2). However the general trends obtained for CONF 1 and CONF 2 are also true for injection configuration CONF 3. Results obtained with injection configuration CONF 4 are presented in Fig. 5. The results indicate an increase in film cooling effectiveness with increasing blowing rate. However for the highest blowing rate M=3.0 a decrease of film cooling effectiveness can be observed for S/D<40. The distributions obtained with CONF 5 (Fig. 5) indicate generally an increase in film cooling effectiveness with increasing blowing rate.

Injection configuration CONF 1 achieves at low and moderate momentum flux ratios higher or similar film cooling effectiveness values than the shaped injection configurations. At higher momentum flux ratios the shaped injection configurations achieve higher film cooling effectiveness levels than injection configuration CONF 1. It should be noted that the coolant consumption of injection configuration CONF 1 is about double compared to the other configurations because of the different hole spacing. Results obtained with compound angle injection (CONF 3) indicate generally a low blowing rate dependency and achieve therefore higher film cooling effectiveness values at higher blowing rates compared to corresponding in-line injection results (CONF 2). However at a streamwise distance of S/D=100 results obtained with CONF 2 and CONF 3 are similar. The results obtained with shaped holes (CONF 4 and CONF 5) indicate an improved film cooling effectiveness due to the laid back angle (CONF 5). This is especially true at higher momentum flux ratios.

Constant heat flux measurements were conducted to determine the local heat transfer coefficients for selected injection configurations (CONF 1 and CONF 4). During these experiments a thin heating foil was glued onto the surface that generated a heat flux directed from the wall into the free-stream fluid. The heat flux is dependent on the local heat transfer coefficient and the difference between the local wall temperature and the local gas temperature close to the wall. In the case of coolant injection the gas temperature can be considered as a mixing temperature resulting from the mixing process of coolant and free-stream gas. To avoid the difficulty to determine this mixing temperature when coolant and free-stream are at different temperatures, both temperatures were adjusted to the same temperature level (T_g=T_c). The reference heat transfer measurements without film cooling were conducted with closed film cooling holes (smooth surface).

The heat transfer results are presented here in terms of Stanton number distributions

$$St_f = \frac{h_f}{c_{pf}\rho_f U_g}\ , \qquad (6)$$

were h_f and U_g are the local values for the heat transfer coefficient and the free-stream velocity respectively. In the case of CO_2 injection the values for the specific heat c_{pf} and density ρ_f are changing in streamwise direction because of the mixing between the coolant and free-stream fluids. To calculate adequate values for c_{pf} and ρ_f corresponding adiabatic film cooling effectiveness results were used. The mixing of CO_2 and the free-stream air was calculated by applying the analogy of heat and mass transfer (Shadid and Eckert [5]). Hence the film cooling effectiveness can be expressed in terms of a concentration ratio of coolant to free-stream for incompressible flows

$$\eta_{ad} = \frac{T_{rg} - T_{aw}}{T_{rg} - T_c} \approx \frac{C_g^{CO_2} - C_w^{CO_2}}{C_g^{CO_2} - C_c^{CO_2}}\ . \qquad (7)$$

With the CO_2 concentrations in the free-stream ($C_g^{CO_2} = 0$) and in the coolant ($C_c^{CO_2} = 1$) the local CO_2 concentration at the wall ($C_w^{CO_2}$) can be directly estimated from the local adiabatic film cooling effectiveness values. The local fluid properties of the air/CO_2-mixture can thus be determined to calculate the appropriate Stanton numbers.

Fig. 6 shows the ratios of Stanton numbers obtained with film cooling to the corresponding Stanton numbers obtained without film cooling. Values above one would indicate that the heat transfer is increased due to coolant injection. Lateral averaged values obtained with CO_2 injection are presented as a function of the streamwise distance S/D. The left graph in Fig. 6 shows the Stanton number ratios obtained with injection configuration CONF 1. Coolant injection causes generally small effects on the

external heat transfer. However, the Stanton number ratios are increased with increasing blowing rate. For the highest blowing rate (M=2) investigated the Stanton number ratio in the near injection region is increased by $St_{f,la}/St_{0,la} \approx 1.16$. Further downstream the distributions decay with increasing streamwise distance to a level of $St_{f,la}/St_{0,la} \approx 0.95$. The Stanton number ratios obtained for CONF 4 are shown in Fig. 6 (right graph). The Stanton number ratios indicate very little sensitivity due to coolant injection within the investigated range of blowing rates ($1 \leq M \leq 3$). Generally a small reduction of the Stanton number ratios due to coolant injection can be observed.

As mentioned before the current film cooling experiments were performed with air and CO_2 as coolant fluids to achieve a variation of the coolant to free-stream density ratio. CO_2 injection has been introduced in experimental investigations to simulate density ratios typically found in gas turbines. Experimental investigations by Teekaram et al. [6] and Jones [7] gave confidence that measurements with CO_2 injection perform a good simulation of those boundary conditions. According to Jones [7] one should account for property effects in order to match air and CO_2 injection results. Based on the analogy between heat and mass transfer an appropriate correction for the adiabatic film cooling effectiveness was derived

$$\eta_{ad}^{F} = \frac{c_{pc}\,\eta_{ad}}{c_{pg}\,(1-\eta_{ad}) + c_{pc}\,\eta_{ad}}, \qquad (8)$$

were η_{ad} is the adiabatic film cooling effectiveness measured with air, c_{pg} is the specific heat of the free-stream fluid and c_{pc} is the specific heat of the coolant fluid.

Pedersen et al. [8] found that the ratio of adiabatic film cooling effectiveness and blowing rate obtained for different density ratios correlate versus the momentum flux ratio. Fig. 7 presents lateral averaged film cooling effectiveness results obtained for air and CO_2 injection according to this method. Note the different scaling of the graphs for different S/D positions. The results obtained with air injection were corrected with respect to eq. (8). A remarkable correlation of the different density ratio results can be observed for all investigated injection configurations.

The related heat transfer results obtained for air and CO_2 injection are also presented as functions of the momentum flux ratio (Fig. 8). The effects of different properties were taken into account by transferring the heat transfer coefficients into Stanton numbers. However, the very small effect due to differences in local Prandtl numbers was neglected. In general a good qualitative correlation of these distributions versus the momentum flux ratio can be observed. However, the results obtained with air injection indicated slightly greater Stanton number ratios than those obtained with CO_2 injection. Independent of the injection configuration an offset of 5% to 10% can be observed at S/D=10, which diminishes with increasing downstream distance.

4. INFLUENCE OF FREE-STREAM ACCELERATION

The film cooling results for each blowing rate obtained for favourable pressure gradient flow were related to the corresponding data for zero pressure gradient flow. These ratios show directly the influence of the free-stream acceleration relative to the non accelerated case.

Fig. 9 shows the film cooling effectiveness ratios obtained for the investigated injection configurations with CO_2 injection. The distributions of injection configurations CONF 1 indicate the strongest increase far downstream (S/D=100) where the film cooling effectiveness is increased by about 30% to 60%. With increasing blowing rate this improvement in film cooling effectiveness due to free-stream acceleration is reduced. The ratios of film cooling effectiveness obtained for CONF 3 indicate also a significant increase in film cooling effectiveness. In contrast to CONF 1 the strongest increase is found close to the injection location, which is followed by a moderate decay of these distributions with downstream distance. At S/D=100 the film cooling effectiveness is still increased by about 40% to 60%. A small decrease of this positive acceleration effect for increasing blowing rate can be observed. Film cooling effectiveness ratios obtained with CONF 4 and CONF 5 show also an increase in film cooling effectiveness due to free-stream acceleration. At S/D=100 the ratios of CONF 4 indicate an increase of 5% - 30%. A moderate decay of these distributions with downstream distance and a moderate decrease of the positive acceleration effect with increasing blowing rate can be observed. Film cooling effectiveness ratios derived from injection configuration CONF 5 indicate a

stronger blowing rate dependency than CONF 4. At S/D=100 the ratios indicate an increase due to free-stream acceleration of 45% for the lowest blowing rate (M=1.0) With increasing blowing rate a decrease of this improvement can be observed. The distribution for the highest blowing rate investigated (M=3.0) indicates a small reduction of film cooling effectiveness due to free-stream acceleration for S/D>70.

Free-stream acceleration caused generally an increase in adiabatic film cooling effectiveness on the concave test surface for the investigated injection configurations and boundary conditions. This effect is more pronounced for the results obtained with cylindrical holes. The positive influence of the free-stream acceleration was attributed to a reduction of the negative curvature influence on the concave surface. The destabilising effects of concave curvature are partly compensated by the stabilising effects of the favourable free-stream pressure gradient flow.

The heat transfer results obtained with favourable pressure gradient flow show similar trends as the corresponding results, which were obtained at zero pressure gradient flow. Hence no significant effects due to free stream acceleration could be derived for injection configurations CONF 1 and CONF 4 (Fig. 10).

Most of above mentioned adiabatic results show a nearly constant increase of film cooling effectiveness downstream of injection. Moreover for some injection configurations a dependency of the blowing rate was observed. Therefore the scaling method introduced by Hartnett et al [9] and applied in two earlier investigations on convex surfaces (Lutum et al. [2] and Lutum et al. [3]) was not applicable. As a consequence of that the following scaling method was introduced to account for effects of the free-stream acceleration on adiabatic film cooling effectiveness on the concave surface

$$\eta^{*}_{ad,la} = C_v \eta_{ad,la} I^{E_v} . \qquad (9)$$

A least square method was used to determine the parameter C_v and E_v for the different injection configuration results separately and are summarised in Tab. 1. Fig. 11 compares the scaled results obtained for favourable pressure gradient flow with results obtained for zero pressure gradient flow. In general a good agreement is found. The small values of E_v determined for CONF 3 and CONF 4 indicate the very small sensitivity with respect to the momentum flux ratio for these injection configurations. Configurations CONF 1 and CONF 5 show a moderate reduction of film cooling effectiveness with increasing momentum flux ratio, which is reflected by increased values of E_v.

Injection configuration	Concave (R/D=-150)	
	C_v	E_v
CONF 1	0.79	0.07
CONF 3	0.62	0.02
CONF 4	0.82	0.01
CONF 5	0.76	0.13

Tab. 1: Parameter used in eq. (9) to account for free-stream acceleration effects on adiabatic film cooling effectiveness on concave surfaces

5. FILM COOLING PERFORMANCE

The previously presented results provide separate information about the film cooling performance in terms of the adiabatic film cooling effectiveness values and the heat transfer coefficients. In general a film injection causes a lower wall temperature but increases the heat transfer coefficient. To determine the quality of a film cooling configuration these two pieces of information have to be considered at the same time. The ratio of the heat fluxes with and without film cooling can be expressed with equations (3) and (5) as

$$\frac{\dot{q}_f}{\dot{q}_0} = \frac{h_f}{h_0} \frac{(T_{aw} - T_w)}{(T_{rg} - T_w)} . \qquad (10)$$

With the definition of the adiabatic film cooling effectiveness and a dimensionless wall temperature Θ this ratio can be expressed as

$$\frac{\dot{q}_f}{\dot{q}_0} = \frac{h_f}{h_0}\left(1 - \eta_{ad}\Theta\right) \tag{11}$$

with

$$\Theta = \frac{T_{rg} - T_c}{T_{rg} - T_w} \ . \tag{12}$$

The dimensionless wall temperature Θ describes the boundary conditions of the cooling process. By setting a reasonable value for Θ=1.5, with the determined values for the adiabatic film cooling effectiveness and the heat transfer coefficient, the heat flux ratio $\dot{q}_f / \dot{q}_o$ can easily be calculated. As the ratio $\dot{q}_f / \dot{q}_o$ is different for each injection configuration and varies with the blowing rate it can be seen as an indicator of the film cooling quality at a certain blowing rate. Heat flux ratios below 1 indicate a reduction of the heat flux into the surface that needs to be cooled.

Fig. 12 and Fig. 13 present the lateral averaged heat flux ratios determined for injection configurations CONF 1 and CONF 4 at the free-stream and coolant boundary conditions investigated. Each graph contains results for a constant coolant density ratio. Fig. 11 shows the heat flux ratios obtained with CONF 1 for air and CO_2 injection. As expected from the discussion in the previous paragraphs the heat flux ratios derived from the accelerated free-stream data (K_g>0) indicated a better film cooling performance as the corresponding data for a zero pressure gradient flow (K_g=0). This is generally true for the results obtained with air injection and also for CO_2 injection for S/D<40. Best film cooling performance with CONF 1 is achieved for the lower blowing rates (M=0.5 and M=1.0). A further increase of the blowing rate does not improve the film cooling performance of the cylindrical holes. The heat flux ratios obtained with CONF 4 are presented in Fig. 13. The air injection results indicate generally slightly better film cooling performance for the case of favourable pressure gradient flow (K_g>0) for S/D<70. An increase of the blowing rate for 1≤M≤2 improves the film cooling performance. At the highest blowing rate investigated (M=3) a decrease in film cooling performance occurred. This decrease is strongest in the near injection region and disappears with downstream distance. The heat flux ratios obtained with CO_2 injection indicate similar trends as the corresponding air injection results. The effect of the free-stream acceleration is less beneficial and appears only in the near injection region.

A comparison of the heat flux ratios obtained with cylindrical and shaped holes show the benefit of the shaped holes clearly. Especially in view of the coolant fluid consumption at the same blowing rate, which is about double for CONF 1 compared to CONF 4 because of the different hole spacing ($P/D_{CONF\ 1}$=3 and $P/D_{CONF\ 4}$=6).

CONCLUSION

Film cooling experiments with a concave test section were conducted with zero and favourable pressure gradient flow. Adiabatic film cooling effectiveness values were obtained with five injection configurations. Additionally heat transfer coefficients were derived for selected injection configurations CONF 1 (cylindrical holes) and CONF 4 (shaped holes). Air and CO_2 were used as coolant fluids to achieve a variation of the density ratio.

The film cooling effectiveness obtained with shaped injection holes achieved generally higher values than cylindrical injection holes for the same hole spacing. This was especially true at higher momentum flux ratios at those strong jet separation occurred for cylindrical hole injection. Results obtained with injection configuration CONF 3, cylindrical holes with compound angle, achieved higher film cooling effectiveness values especially at higher blowing rates compared to corresponding results from CONF 2 (in-line injection). However at a streamwise distance of S/D=100 results obtained with CONF 2 and CONF 3 were similar. The results obtained with shaped holes indicated an improved film cooling effectiveness due to the laid back angle (CONF 5). This was especially true at higher blowing rates.

Free-stream acceleration caused generally an increase in adiabatic film cooling effectiveness on the concave test surface for all investigated injection configurations and boundary conditions.

The effect on the heat transfer coefficients was in general small. The variation of the Stanton number ratios with the blowing rate was more pronounced for cylindrical holes than with shaped holes.

The free-stream acceleration indicated no significant effects on the Stanton number distributions determined during these heat transfer experiments with film cooling on the concave test surface.

ACKNOWLEDGEMENT

This work was carried out within the Brite EuRam project “Turbine Aero-Thermal External Flows” (BE97-4440) and was sponsored by the *Bundesamt für Bildung und Wissenschaft* (Switzerland). The authors wish to acknowledge the fruitful collaboration with their partners within this project and their permission to publish this paper. Additionally the authors would like to thank ALSTOM Ltd. for their permission to publish the paper.

REFERENCES

1. E. Lutum, J. von Wolfersdorf, B. Weigand and K. Semmler (2000) Film Cooling on a Convex Surface with Zero Pressure Gradient Flow. Int. Journal of Heat and Mass Transfer **43**: 2973-2987
2. E. Lutum, J. von Wolfersdorf, K. Semmler, J. Dittmar and B. Weigand (2001) Film Cooling on a Convex Surface with Favourable Pressure Gradient Flow. Accepted for publication in Int. Journal of Heat and Mass Transfer **44**: 939-951
3. Lutum, E., von Wolfersdorf, J., Semmler, K., Naik, S. and Weigand, B. (2001) Film Cooling on a Convex Surface: Influence of External Pressure Gradient and Mach Number on Film Cooling Performance. Accepted for publication in J. Heat and Mass Transfer
4. Moffat, R. J (1988) Describing the Uncertainties in Experimental Results. Experimental Thermal and Fluid Science, **1**: 3-17
5. Shadid J. N. and Eckert E. R. G. (1991) The Mass Transfer Analogy to Heat Transfer Fluids With Temperature-Dependent Properties. Journal of Turbomachinery **113:** 27-33
6. Jones, T. V. (1999) Theory for the Use of Foreign Gas in Simulating Film Cooling. Int. Journal of Heat and Fluid, **20**: 349-354
7. Teekaram, A. J. H., Forth, C. J. P. and Jones, T. V. (1988) The Use of Foreign Gases to Simulate the Effects of Density Ratios in Film Cooling. ASME Paper 88-GT-37
8. Pedersen, D. R., Eckert, E. R. G. and Goldstein, R. J. (1977) Film Cooling with Large Density Differences Between the Mainstream and the Secondary Fluid Measured by the Heat-Mass Transfer Analogy. ASME Journal of Heat Transfer, **99**: 620-627
9. Hartnett, J. P. and Birkebak, R. C. and Eckert, E. R. G., “Velocity Distributions, Temperature Distributions, Effectiveness and Heat Transfer in Cooling of a Surface with a Pressure Gradient”, Int. Development in Heat Transfer, Part 4, ASME, pp. 682-689, 1961.

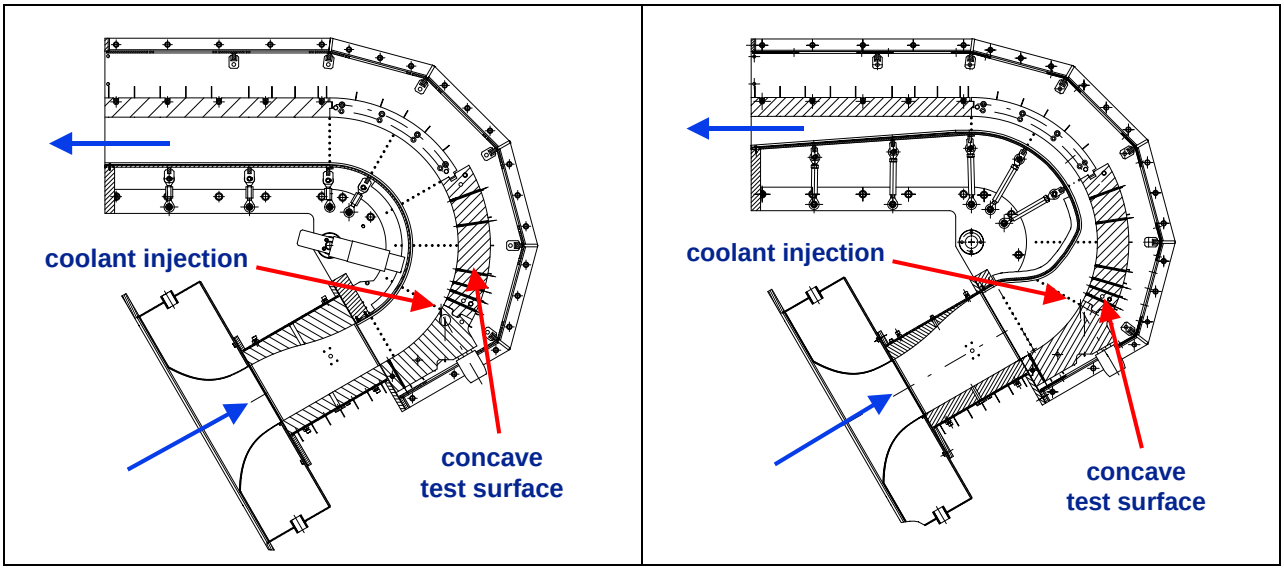

Fig. 1: Concave test sections, left: zero pressure gradient flow and right: favourable pressure gradient flow

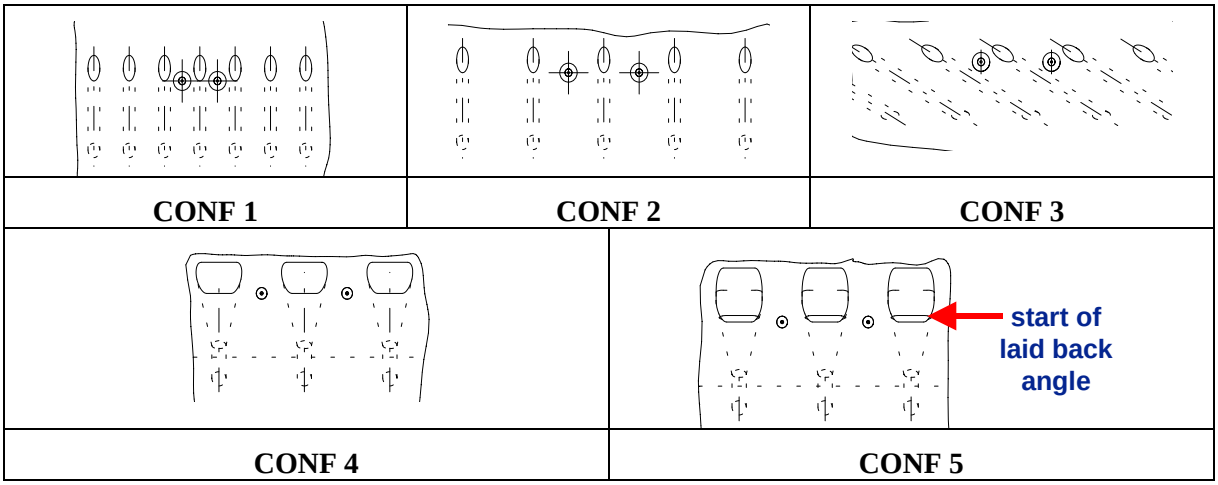

Fig. 2: Cylindrical and shaped film cooling hole geometries

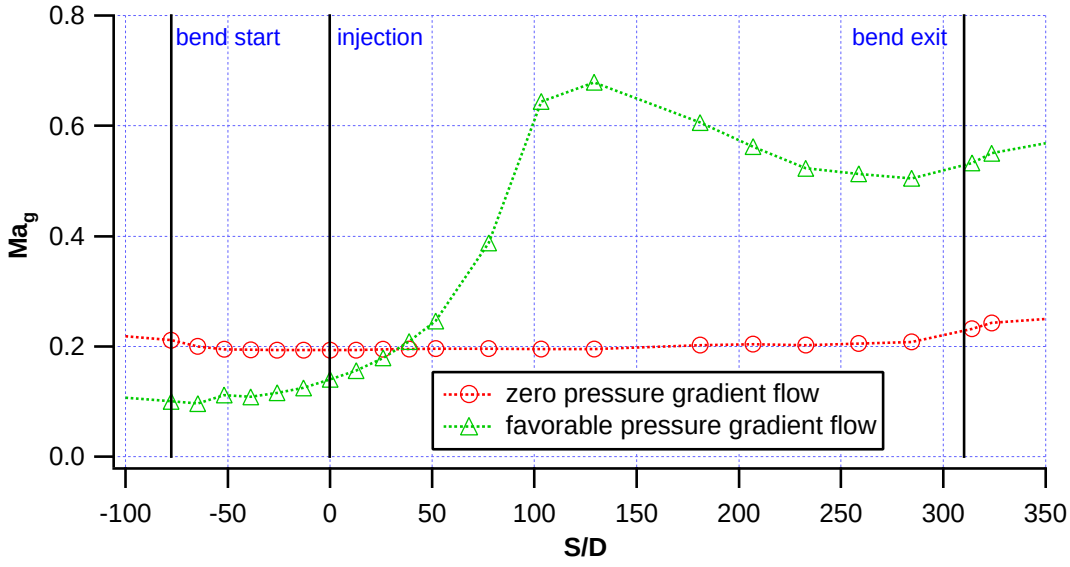

Fig. 3: Distributions of isentropic Mach number versus streamwise distance along the concave test surface

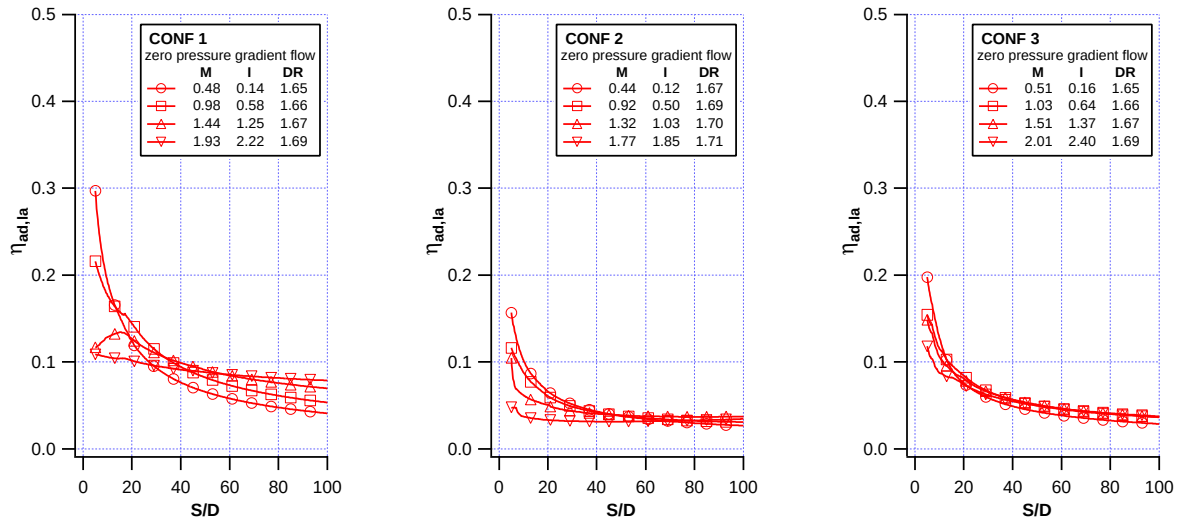

Fig. 4: Distributions of lateral averaged film cooling effectiveness values obtained for cylindrical injection configurations (CONF 1, CONF 2 and CONF 3) at zero pressure gradient flow

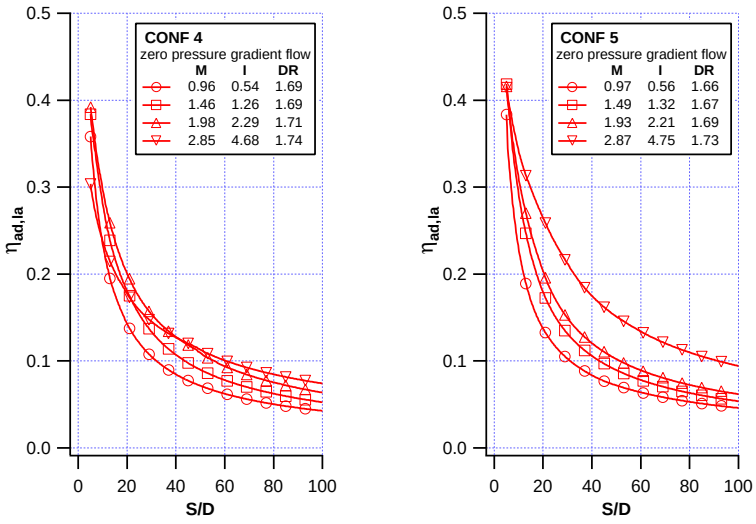

Fig. 5: Distributions of lateral averaged film cooling effectiveness values obtained for shaped injection configurations (CONF 4 and CONF 5) at zero pressure gradient flow

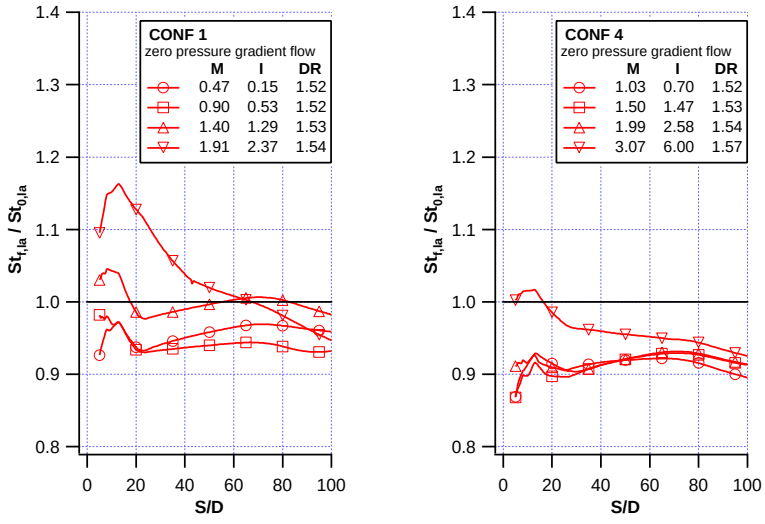

Fig. 6: Distributions of lateral averaged Stanton number ratios obtained for cylindrical (CONF 1) and shaped (CONF 4) injection configurations at zero pressure gradient flow

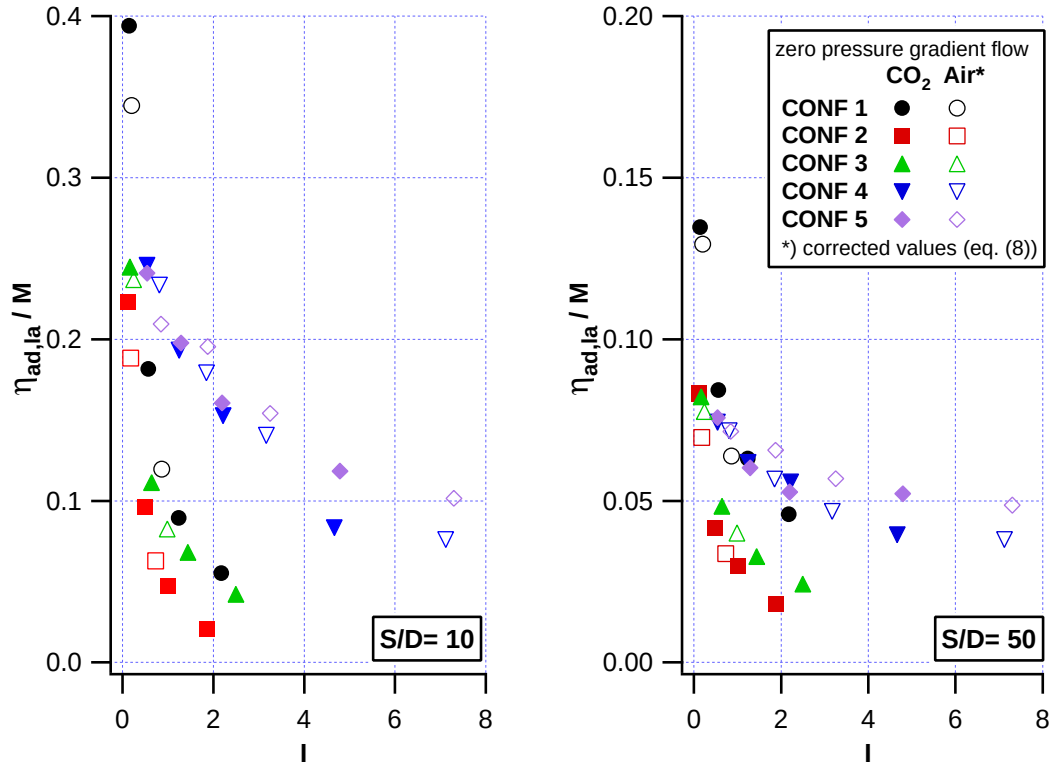

Fig. 7: Compensation of density ratio effect on lateral averaged adiabatic film cooling effectiveness for investigated injection configurations

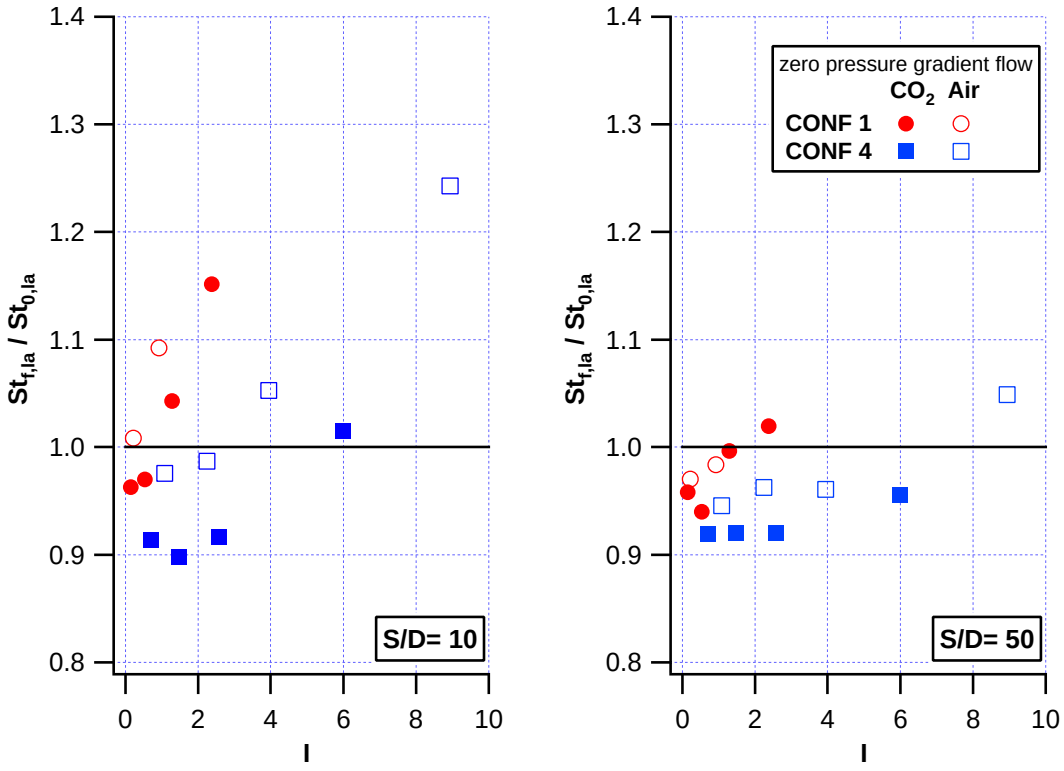

Fig. 8: Distributions of lateral averaged Stanton number ratios versus momentum flux ratio obtained for air and CO_2 injection for cylindrical (CONF 1) and shaped (CONF 4) injection configurations

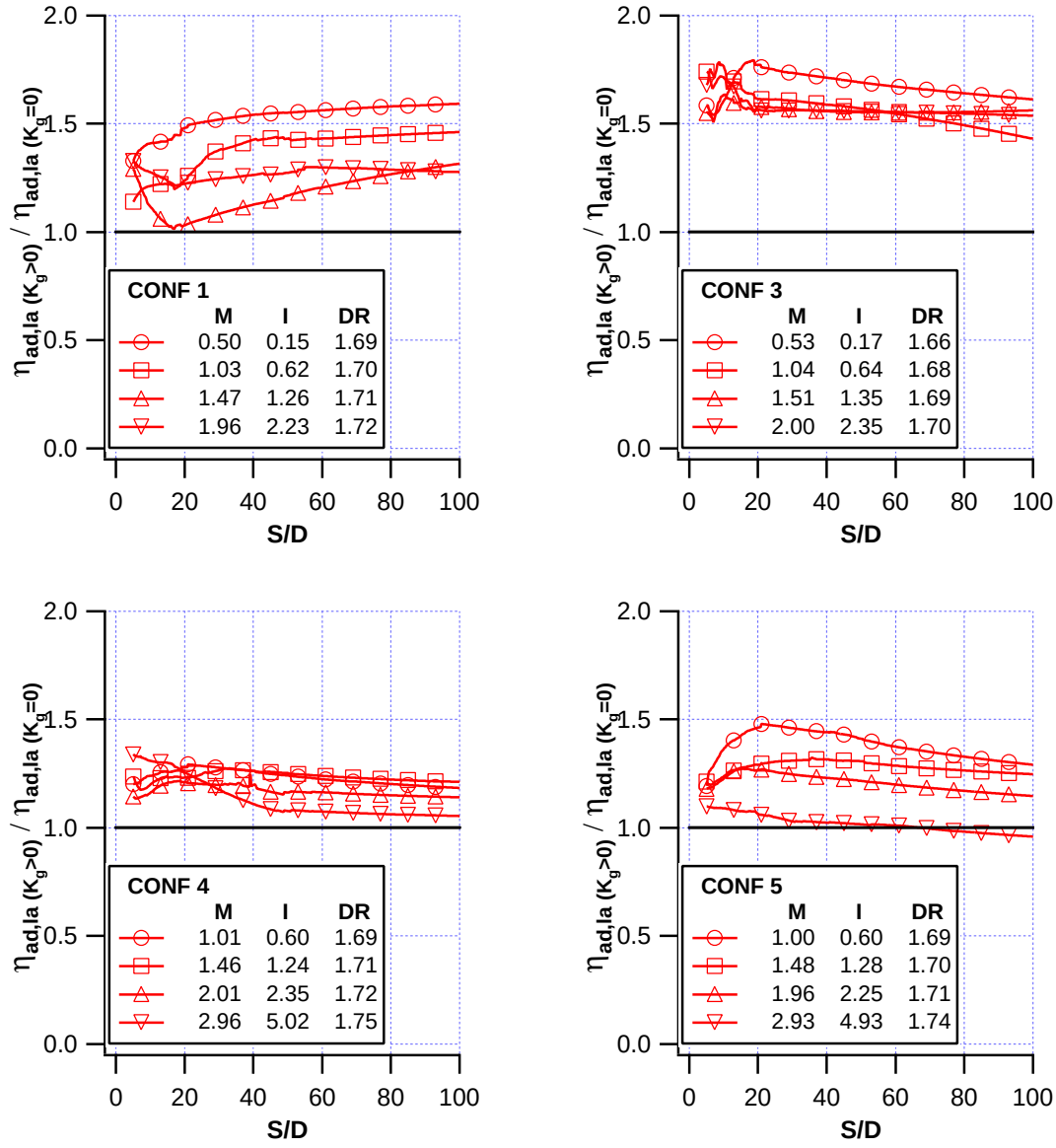

Fig. 9: Distributions of lateral averaged adiabatic film cooling effectiveness ratios obtained for zero and favourable pressure gradient flow for cylindrical (CONF 1 and CONF 3) and shaped (CONF 4 and CONF 5) injection configurations

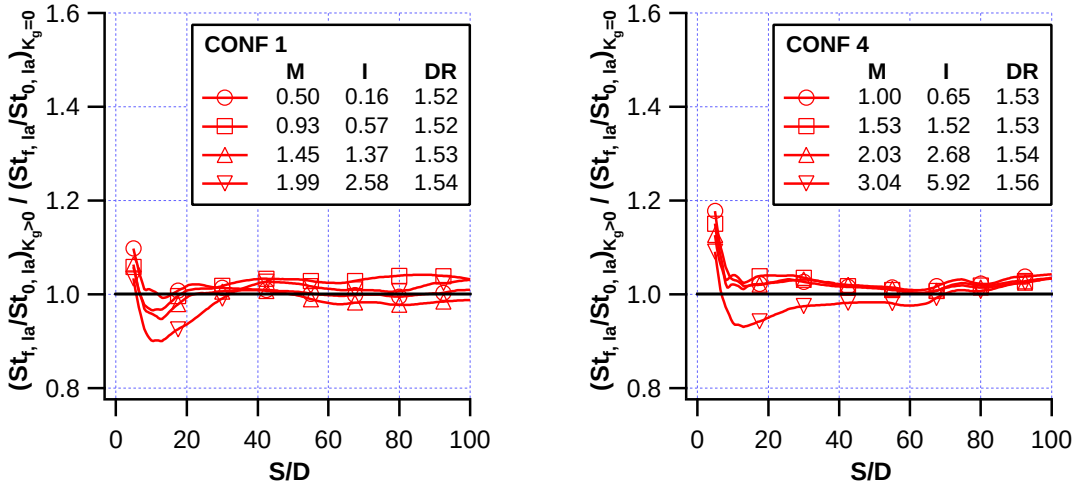

Fig. 10: Distributions of lateral averaged Stanton number ratios obtained for zero and favourable pressure gradient flow for cylindrical (CONF 1) and shaped (CONF 4) injection configurations

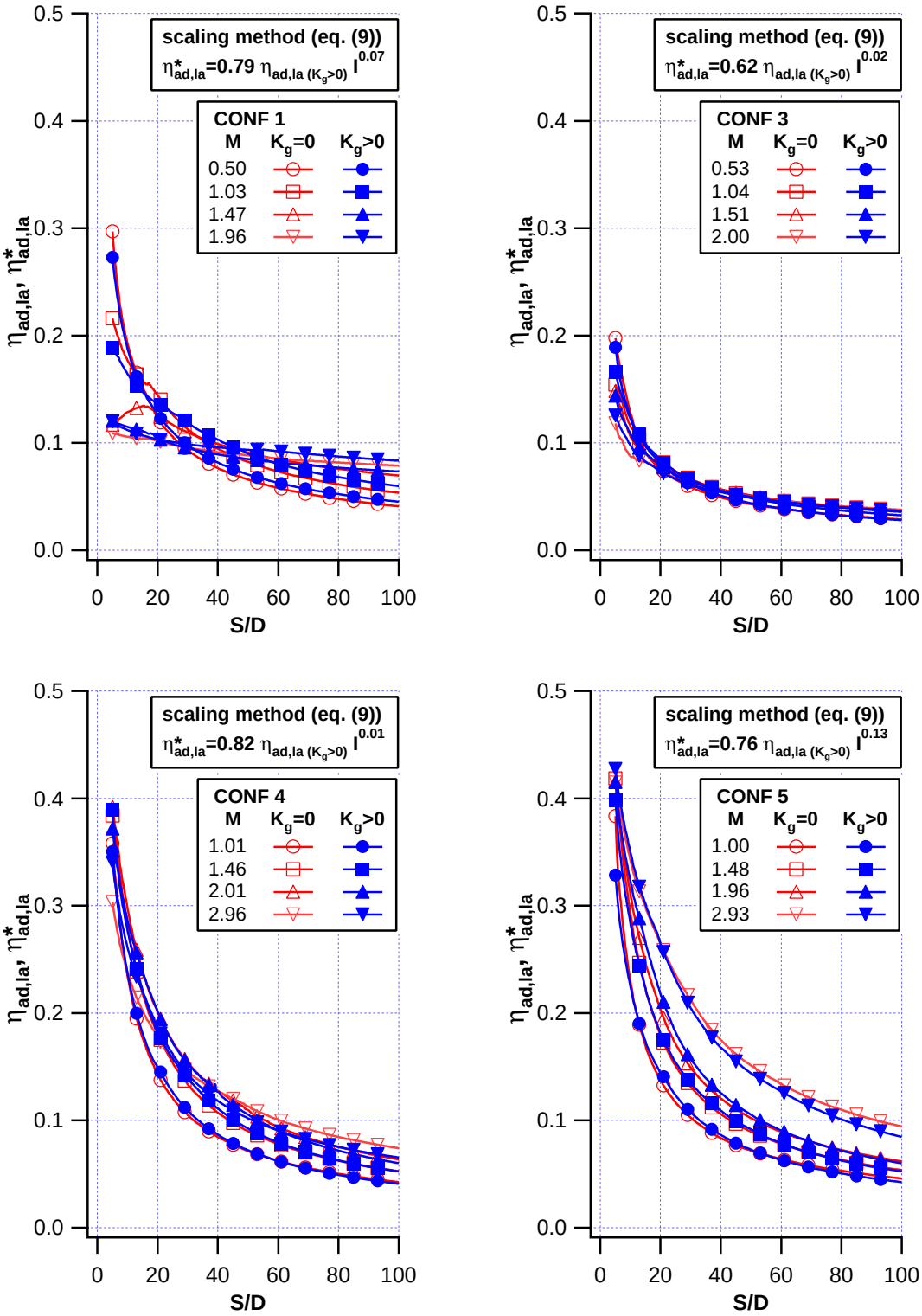

Fig. 11: Correlation method (eq. (9)) to account for the effect of free-stream acceleration on lateral averaged adiabatic film cooling effectiveness for cylindrical (CONF 1 and CONF 3) and shaped (CONF 4 and CONF 5) injection configurations

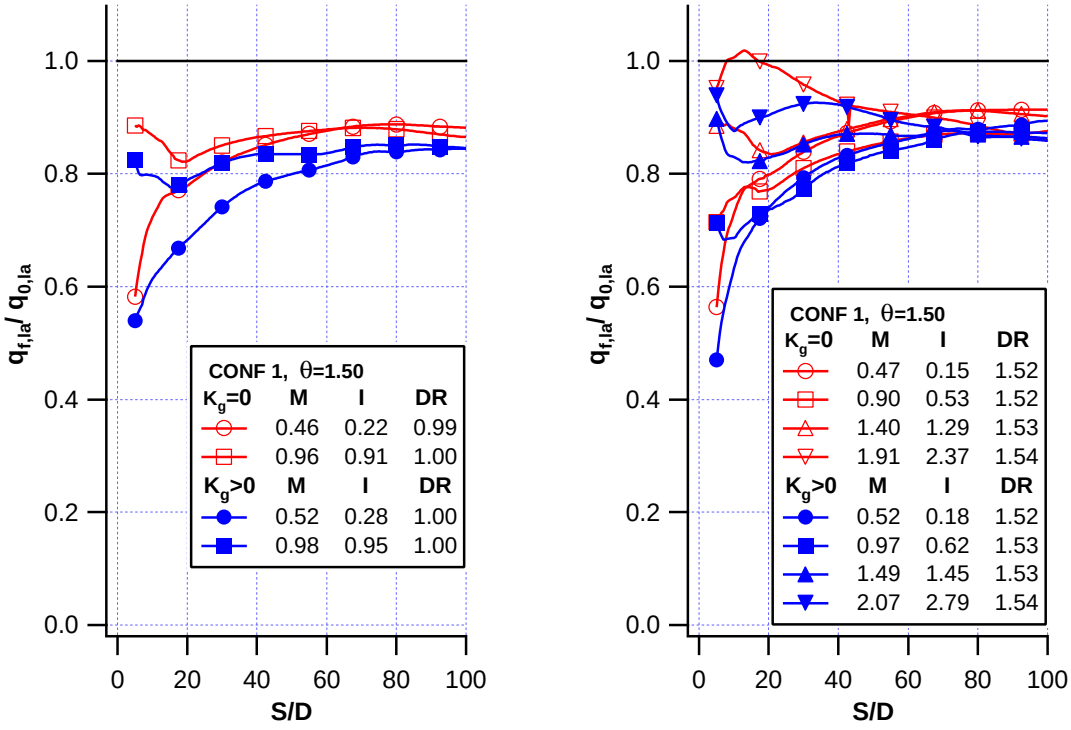

Fig. 12: Distributions of heat flux ratios obtained for zero and favourable pressure gradient flow for cylindrical film holes (CONF 1); air (left) and CO_2 (right) injection

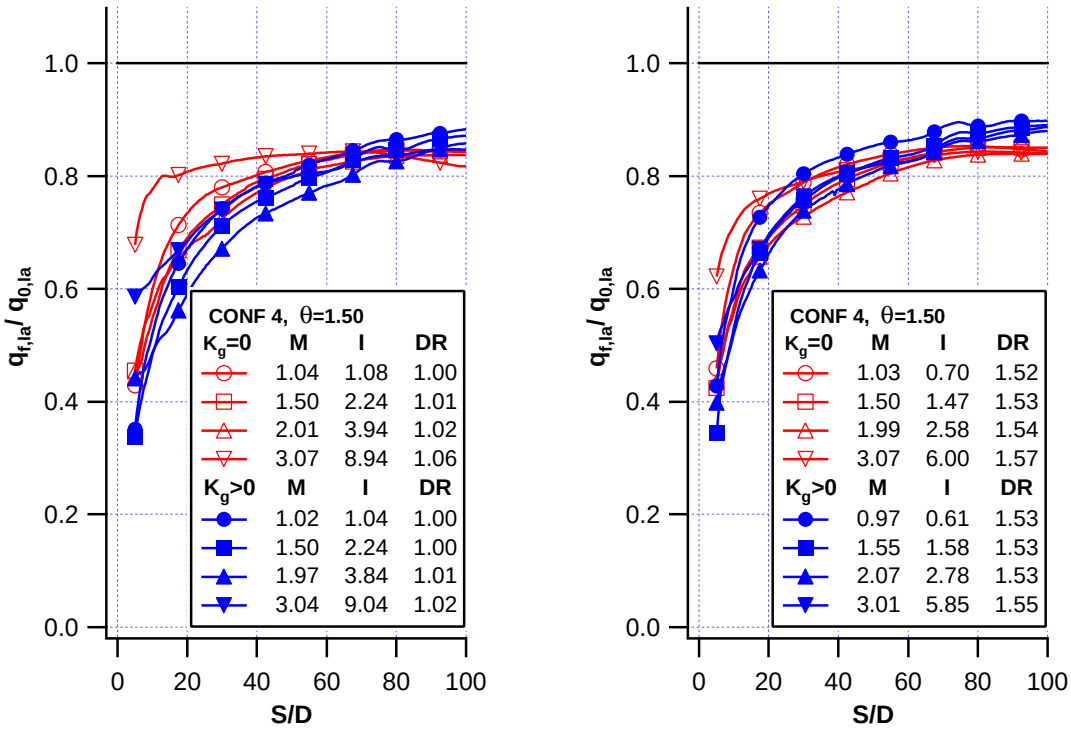

Fig. 13: Distributions of heat flux ratios obtained for zero and favourable pressure gradient flow for shaped film holes (CONF 4); air (left) and CO_2 (right) injection

Paper Number: 7

Name of Discusser: S. Wolff, Universität Bundeswehr Munich

Question:
Comparison between results with and without film cooling. Are the reference measurements performed with or without film cooling holes?

Answer:
The film cooling holes were taped during test without coolant injection to achieve a smooth surface.

Name of Discusser: H.B. Weyer, DLR Cologne

Question:
1) Have you observed any effect of the vortex typical for curved channels?
2) Did you compare the experimental results with numerical simulation for clarifying the mechanisms of film cooling?

Answer:
1) We did not observe these kind of flow features on the concave wall, which was most likely due to the high. Rexnolds number and turbulence intensity of the free stream flow.
2) So far we did not compare these experimental results with numerical simulations. Our experiments with CFD for other test cases show quite poor agreement with experimental results in terms of film cooling effectiveness. But we might consider this to investigate the flow field feature which would allow to draw some conclusions regarding the film cooling results.